NANO LETTERS

pubs.acs.org/NanoLett
Letter

Synergistic Biofilter Tube for Promoting Scarless Tendon Regeneration

Renhao Yang,[§] Yidong Xu,[§] Renxuan Li,[§] Yin Zhang, Yang Xu, Liuquan Yang,* Wenguo Cui,* and Lei Wang*

Cite This: *Nano Lett.* 2024, 24, 7381−7388
Read Online

ABSTRACT: Inspired by the imbalance between extrinsic and intrinsic tendon healing, this study fabricated a new biofilter scaffold with a hierarchical structure based on a melt electrowriting technique. The outer multilayered fibrous structure with connected porous characteristics provides a novel passageway for vascularization and isolates the penetration of scar fibers, which can be referred to as a biofilter process. In vitro experiments found that the porous architecture in the outer layer can effectively prevent cell infiltration, whereas the aligned fibers in the inner layer can promote cell recruitment and growth, as well as the expression of tendon-associated proteins in a simulated friction condition. It was shown in vivo that the biofilter process could promote tendon healing and reduce scar invasion. Herein, this novel strategy indicates great potential to design new biomaterials for balancing extrinsic and intrinsic healing and realizing scarless tendon healing.

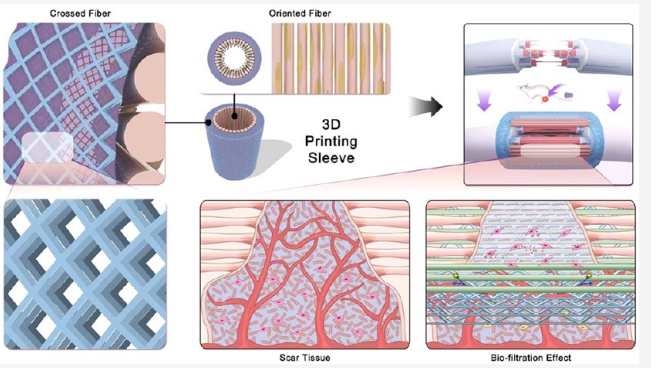

KEYWORDS: *biomedical melt electrowriting, biofilter effects, hierarchical structure, scarless tendon healing*

Tendon tissue is a crucial part of the musculoskeletal system, responsible for connecting muscle and bone tissue and facilitating mechanical conduction.[1] A tear, whether partial- or full-thickness, often leads to the disruption of tendon continuity. Thus, patients would experience significant impairment in joint and limb mobility, leading to a detrimental effect on the quality of life. The regeneration of the tendon follows the conventional process of tissue repair, which includes inflammation, reparation (scarring), and remodeling (late rearrangement of the tendon bundle). Typically, this process is mediated by a combination of extrinsic and intrinsic tendon healing mechanisms: intrinsic healing is associated with the self-proliferation of tenocytes and the formation of an extracellular matrix; extrinsic healing is characterized by the infiltration of fibroblasts and capillaries, while scar repair occurs through the development of new granulation tissue. The biomechanical function and tissue arrangement caused by extrinsic healing are significantly worse than those of a typical tendon.[2] Tendons, being composed of tissue with a limited blood supply and cells, typically undergo a healing process that is primarily driven by extrinsic factors. This involves bringing new blood vessels and active tissue to the repair site. However, excessive scar tissue formation and disorganized fiber deposition often occur with the growth of new blood vessels. These complications can lead to postoperative adhesions, which significantly impair the biomechanical function after surgery.[3] Hence, it is crucial to maintain control of the balance between the competitive dominance of extrinsic and intrinsic healing during the tendon repair process. This coordination ensures that the overall effectiveness of the repair and prevents the growth of scar tissue into the tendon tissue.

During extrinsic healing, the local inflammatory response and recruitment of inflammatory cells lead to fibroblast infiltration, which provides essential nutrients for subsequent tissue repair. Fibrous cells surrounding the tendon can facilitate this process through continuous proliferation. However, the lack of sufficient vascular cells in the primary tendon structure often disturbs the healing process, including scarring and peritendinous adhesions.[4] Currently, various biomaterials, such as electrospun fiber scaffolds and silicone cannulas, are commonly employed to address those issues. However, these methods have limitations, such as low porosity and the lack of regenerative capabilities. Consequently, they can result in inadequate biomechanical repair and postoperation failure.[5] To address the issue of poor regenerative characteristics, chemical modifications, such as mRNA, nanomolecular medicines, and various active components such as liposomes are introduced

Received: April 1, 2024
Revised: May 27, 2024
Accepted: May 28, 2024
Published: June 4, 2024

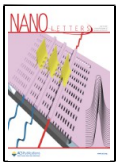

https://doi.org/10.1021/acs.nanolett.4c01540
Nano Lett. 2024, 24, 7381−7388

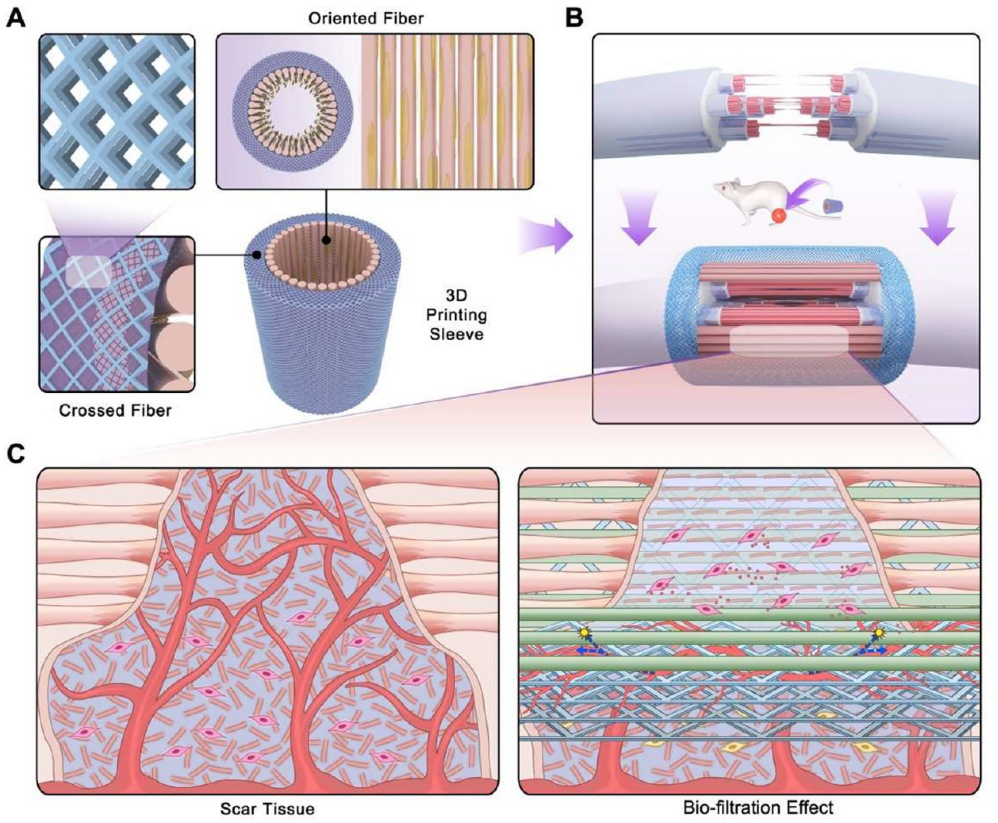

Figure 1. Schematic diagram of the structure and the scarless tendon regeneration effect of the biofilter tube. (A) The structure of the biofilter tube for different directions. (B) The implantation and repair process of the biofilter tube in a rat tendon injury model. (C) The mechanism of the biofilter tube for scarless tendon regeneration, in which the neo fiber was aligned with the orientational scaffold fiber and the neovascularity penetrated in the scaffold and provided a local neovascularization environment.

into the biological scaffold.[6−9] Nevertheless, due to challenges such as biosafety, packaging efficiency, and difficulties in clinical application, chemical modification is not the most effective way to achieve reliable tendon regeneration.

The extrinsic vascular system plays a critical role during the initial phases of tendon healing, i.e,. supplying the local environment with essential nutrients eliminating waste and modulating the immune response.[10] Therefore, it is essential to establish a well-supplied vascular microenvironment around the damaged tissue and regulate the infiltration of the neovascularization. The newly born capillaries are about 6−9 μm in diameter, which is much smaller than the normal 50−80 μm diameter of fibroblasts. It is possible to selectively allow the infiltration of capillaries while suppressing the overinvasion of fibroblasts during the initial phase. This can be achieved by adjusting the structural characteristics (e.g., porosity) of the biological scaffold, achieving biofilter effects. Such topological structures can also determine the cell fate in tissue regeneration with high effectiveness and precision. Adjustments in the local topology of tendon cells, for instance, can lead to adaptive phenotypes, including tenogenic differentiation.[11] The appropriate introduction and amplification of the local stress environment, especially shear stress, can enhance the healing of damaged tissue. It can also boost the self-repair capability of tendons when combined with a biomimetic structure.[12] However, it remains challenging to build a bionic topological structure that combines biological filtration (biofilter effects) with coupled shear force to achieve behavioral regulation at the cellular level and promote tendon tissue regeneration.

The melt electrowriting (MEW) technique, as a high-resolution 3D printing technique, has been widely used for fabricating scaffolds with complex structures.[13,14] It is capable of providing both improved controllable structural and flexible possibilities in filament and material morphology. Therefore, it enables the creation of programmable biological structural scaffolds. In this study, a novel hierarchical anisotropic Janus scaffold was fabricated by MEW, possessing topological structure characteristics for tendon repair (Figure 1). In vitro, the well-aligned fibers inside the scaffold can promote tenocyte-specific bonding and migration. It activates the expression of the mechanical force-related protein Piezo-1 and tenogenesis-related proteins Col-I and SCX in a shear force environment that stimulates relative movement in the body. Simultaneously, it can prevent excessive scar tissue ingrowth in vivo, promote local extracellular matrix deposition, and speed up the rearrangement of the corresponding tendon fibrous tissue. It has been demonstrated in the rat Achilles tendon injury model. Finally, the oriented topological structure in the inner layer contributes to the regeneration of damaged tendon tissue, while the mixed and staggered fiber structure in the outer layer creates a synergistic biofilter effect.

The traditional Janus tube features an asymmetrical morphological structure and chemical composition on both sides, giving the Janus membrane unique biorepairable properties that surpass those of homogeneous materials.[15−17] However, it was hard for this approach to control the membrane thickness and even drug loading efficiency. This study fabricated an integrated Janus structure via MEW with

https://doi.org/10.1021/acs.nanolett.4c01540
Nano Lett. 2024, 24, 7381−7388

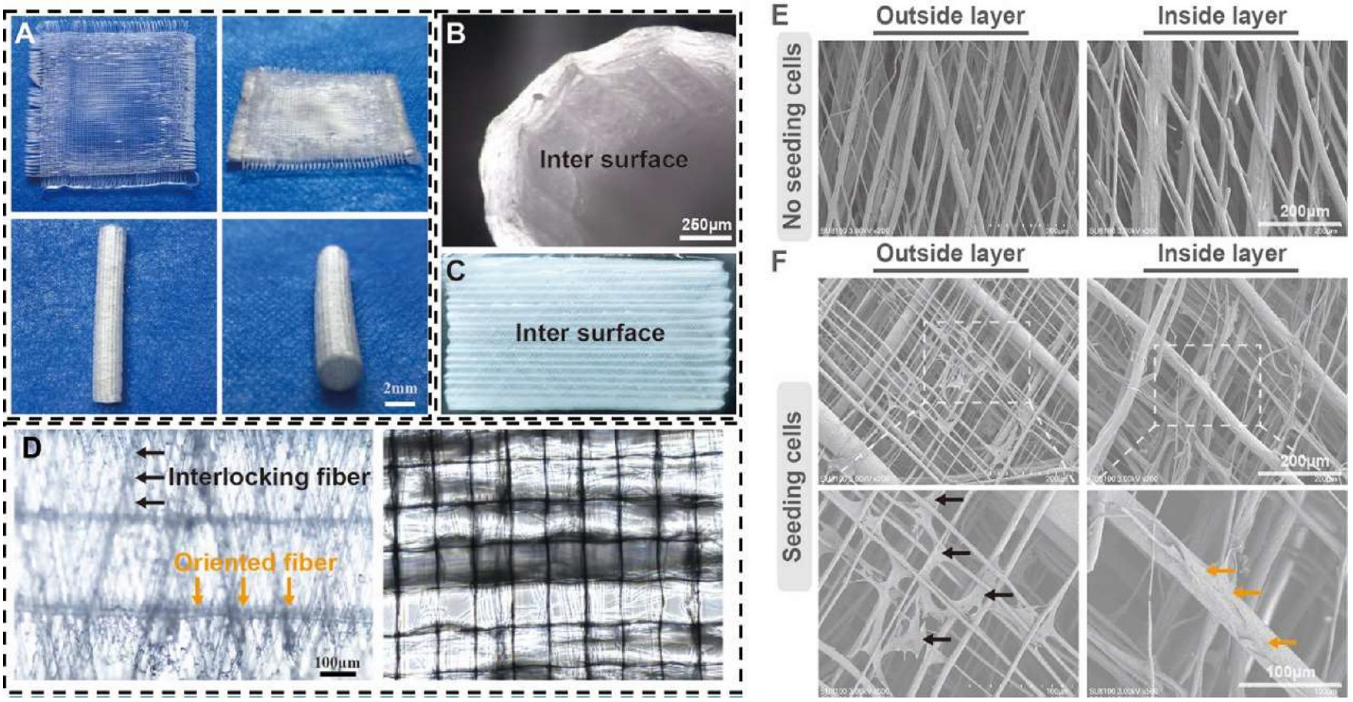

Figure 2. Anisotropic Janus tube scaffold characterization and local morphology. (A) The general morphology of the Janus tube and net patch scaffold. (B) Local architecture of the Janus scaffold. (C) Observation of the morphology of a Janus tube under an optical microscope. (D) SEM micrographs of the Janus tube from different sides. (E,F) SEM micrographs of the Janus tube from different sides after 5 days of cell culturing.

programmable and one-step construction advantages. The general shapes are shown in the Figure 2A. The net patch printing scaffold was consisted of oriented PCL fibers arranged in a perpendicular vertical direction, as control group. The Janus tube was fabricated as a long tube with 3 mm diameter. The outer surface of the tube was composed of interlocking PCL fibers, and the inter surface was constructed from parallel longitudinally orientated fibers which were similar to the tendon fiber arrangement structure. As shown in Figure 2B,C, the original oriented fiber morphology inside the tube and the oriented alignment after unfolding the tube could be better observed. Local structures of the two scaffolds were observed by a light microscope, as shown in Figure 2D. The black arrow marks the interlocking fiber in the outer surface, and the orange arrow marks the oriented fiber in the inter surface. The vertical fiber features were shown in the net patch printing scaffold. In contrast, the Janus tube showed both the interlocking and longitudinally parallel Polycaprolactone (PCL) fibers in the projected vertical shot of the light microscope. Then, the mechanical characterization of the two groups was tested, and there was no significant difference between the two groups (Figure S1).

The microstructure of the Janus tube and net patch scaffold was characterized by SEM. First, there were complete fibers showing interlocking direction in the outside layer and interspersed longitudinal fibers among the interlocking fibers in the inside layer, as shown in Figure 2E. Additionally, the local details of the net patch scaffold are shown in Figure S2. Then, the tenocytes were seeded on the outside layer for culturing 5 days and checked again by SEM. The related results are shown in Figure 2F, where the cells were attached on the outside fiber but did not penetrate the underlying fiber layer. The outside fiber would be thinner than in the preplanting state cause of cellular degradation and erosion on the PCL fiber, which is marked by the black arrows, and the cells were blocked by the interlocking networks of the outer layers. In the inside layer, cells were mainly recruited and attached to the surface of longitudinal fibers and the general morphology of the cells was arranged along the longitudinal direction, which is marked by the orange arrows. So, the outside fiber structure could prevent some cell invasion into the interlocking fiber space.

To verify the biocompatibility of those prepared scaffolds, tenocytes were seeded and cultured on the scaffold surface and live−dead staining. As shown in Figure S3, no cell death was observed in any group after 3 days of culturing, which demonstrated the good biocompatibility of the PCL scaffold system. Furthermore, to investigate the biocompatibility of the PCL scaffold system, tenocytes were seeded on the scaffolds and cultured for 5 days. As shown in Figure 3A, the tenocytes showed random and nondirectional cell distribution on the culture plate. In comparison, the cells grew and attached along the fibers and displayed different orientations. The orientation rates of tenocytes in different culture systems were then analyzed and counted. Compared to the chaotic cellular arrangement on the culture plate, both the net patch scaffold and the Janus tube were able to allow tenocytes to appear in a more oriented arrangement (Figure 3B). Subsequently, cell cultures were performed for different times (5 and 10 days) on the net patch scaffold and the inside surfaces of the Janus tube to observe the cell migration property (Figure 3C). The cells mainly migrated and extended along the longitudinal fibers, and then gradually moved to the interlocking fibers on both sides, which has been reported by other researchers as well.[18−21]

Shear force is present within the tendon as a primary loading mechanism to redistribute load and is important for the tendon development and homeostasis. The tenocytes are mechano-

https://doi.org/10.1021/acs.nanolett.4c01540
Nano Lett. 2024, 24, 7381−7388

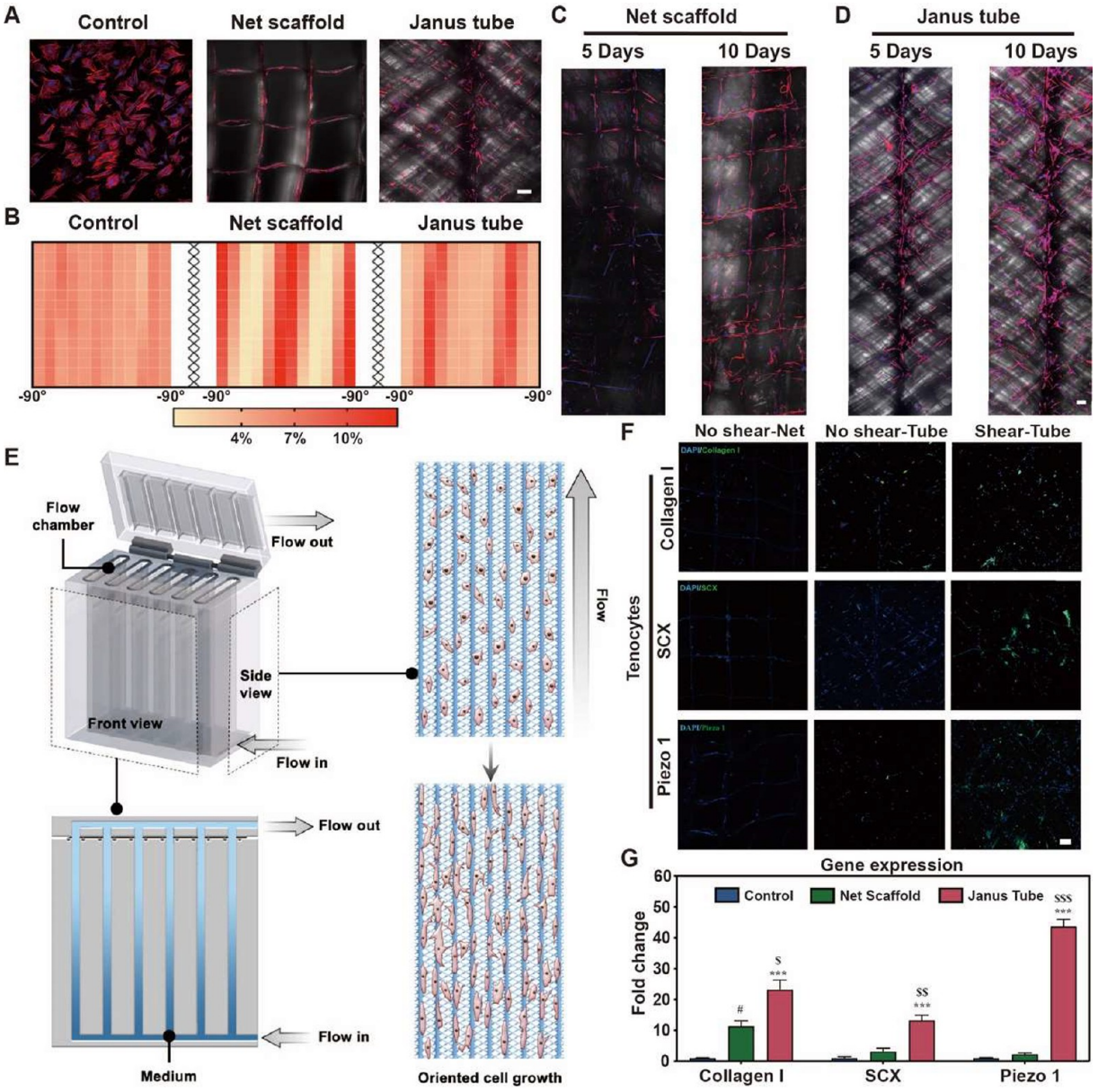

Figure 3. Influence of Janus tube on tenocyte behavior patterns and an in vitro shear simulation test. (A) Cytoskeleton staining in Janus tube and Net scaffold. (B) Cell distribution trend quantification on the scaffold surface. (C,D) Cell migration characteristics at different time points. (E) Schematic diagram of in vitro shear force simulation. (F) Expression of mechanics and tendon formation related proteins among different groups under shear force (bar = 100 μm). (G) Quantitative analysis of in vitro shear modeling (mean ± SD, Janus tube vs control, *** $P < 0.001$; Janus tube vs net scaffold, $ $P < 0.05$, $$ $P < 0.01$, $$$ $P < 0.001$; net scaffold vs control, # $P < 0.05$; $n = 3$).

sensitive to shear stress induced by collagen-fiber sliding in tendons and secrete collagen fiber.[22,23] Currently, to simulate the shear forces on tendon cells, some researchers have cultured cells on a cell culture slide surface and used another glass slide to create friction against the glass slide, thereby simulating the shear stress condition on tenocytes. However, it is difficult to control the stress conditions of cells in this way, and direct physical contact could easily cause direct local cell damage. It may be difficult to obtain stable results and hard to stimulate the shear force applied on the biomaterials.[24,25] To solve the above application challenges, this study innovatively used the Flex400 shear force module to detect the cellular status on the biomaterials via intermittent flushing and regulating the flow rate of the culture medium. In this experiment, the topological structure scaffold seeded with tendon cells was placed along the direction of water flow erosion. Thus, the water flow to simulate shear force erosion can be realized (Figure 3E). First, the tenocytes were seeded on the inside of a Janus tendon tube and cultured for 10 days. Second, the cell-grown Janus tube was put into a shear stress device and the shear environment was simulated by using a continuous medium flow. To further optimize the role of shear forces on tenocytes, immunofluorescence staining was performed to investigate the gene expression, such as Piezo1, ColI, and SCX, which responded to mechanical stress and associated with tendon regeneration,[26,27] as shown in Figure 3F. Compared with the no-stimulation scaffolds, the fluorescence intensities of Piezo1, ColI, and SCX increased under the shear force stimulation (Figure 3G).

https://doi.org/10.1021/acs.nanolett.4c01540
Nano Lett. 2024, 24, 7381−7388

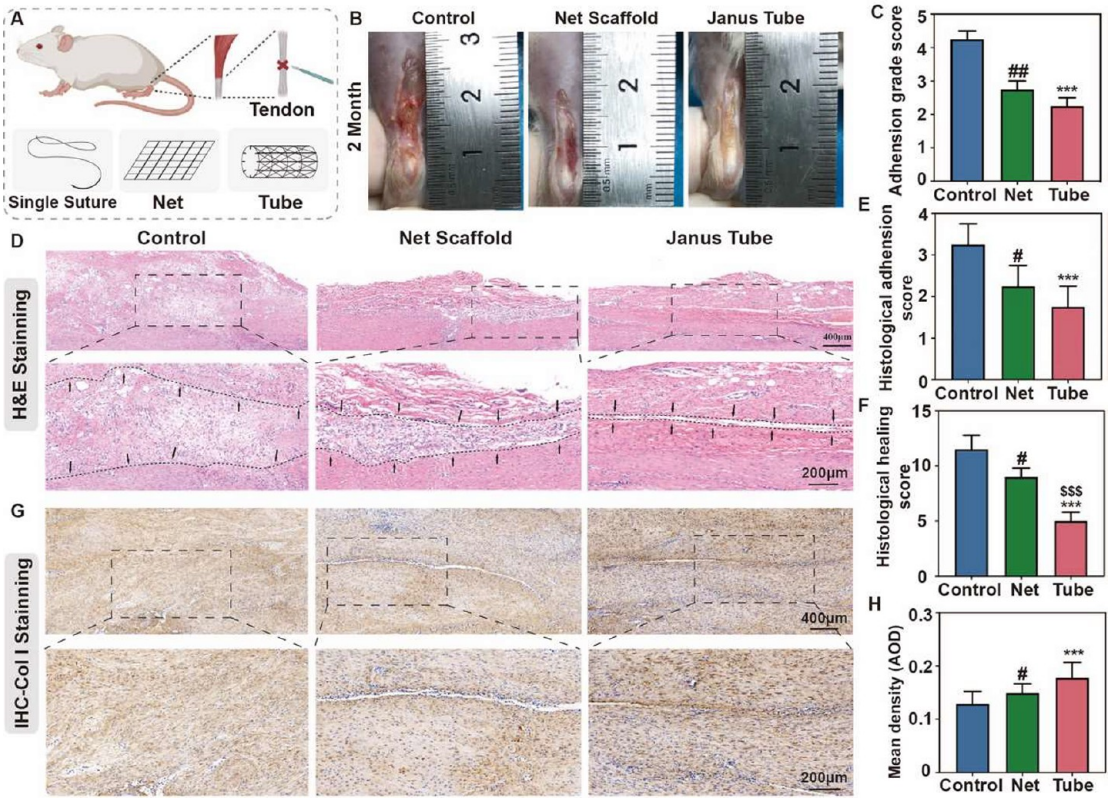

Figure 4. Evaluation repair performances of the Janus tube in vivo. (A) Application of different scaffolds for tendon repair. (B) Gross observation of peritendinous adhesion of injured tendon at 4 weeks. (C) Gross scores of peritendinous adhesion (mean ± SD; Janus tube vs control, *** $P < 0.001$; net scaffold vs control, ## $P < 0.01$; $n = 3$). (D) H&E staining images of different scaffolds. The dotted area showeds the adhesion region. (E,F) Histologic scores of tendon adhesion and tendon healing (mean ± SD, Janus tube vs control, *** $P < 0.001$; Janus tube vs net scaffold, $$$ $P < 0.001$; net scaffold vs control, # $P < 0.05$; $n = 3$). (G,H) Immunohistochemical staining and evaluation of Col I expression in peritendinous tissue at 4 weeks (mean ± SD; Janus tube vs control, *** $P < 0.001$; net scaffold vs control, ## $P < 0.01$; $n = 3$).

As shown in Figure 4A, the ruptured tendon was sutured and subsequently wrapped with a net patch scaffold or a Janus tube to achieve scarless tendon healing. Healing and adhesion grade were assessed by observing the surgical site of the Achilles tendon. The rat Achilles tendon model was divided into three groups: untreated control group, net patch group, and Janus tube group. There were no infectious or necrosis signs around the incision in the three groups. After 4 weeks postoperation, the adhesion of the Janus tube around the peritendinous tissues was rather improved compared with the other groups. In contrast, more dense fibrotic tissue around tendon tissue was observed in the tendon injury suture group and net patch scaffold group (Figure 4B). Notably, there was less jellylike collagen deposited on the tendon surface, which was the adhesive tissue on the upper surface, in the Janus tube groups (Figure 4B). The tendon adhesion evaluation revealed that the adhesion in the control group was mainly distributed between grades 4 and 5. The adhesion grade in the net patch scaffold and the Janus tube group was mainly distributed between 2 and 3, and the improvements were due to the barrier between the scaffold and the peritendinous tissue. Furthermore, the adhesion score of the Janus tube was lower than those of the other two groups, with a statistical difference compared with the control group (Figure 4C).

For further characterization of the tendon adhesions and the effect of histopathological changes, a histopathological staining and histological analysis were performed. First, hematoxylin and eosin (H&E) staining was performed to observe the adhesion on the tendon surface and invasion into the repaired area. As shown in Figure 4D, there was smoother and less adhesion on the tendon surface in the Janus tube group. However, sections from the control group showed much more adhesion tissue depositing on the surface and invading into the repaired area. Furthermore, the histological evaluation of the three groups showed that the Janus tube group had a lower adhesion score than the other two groups, with a statistical difference (Figure 4E). The histological healing score was evaluated to explore the tendon repair potential of different scaffolds. The Janus tube group showed a higher healing score, mainly distributed between grades 4 and 6, compared to the control and net patch groups (Figure 4F). Figure 4G.H showeds that collagen I deposition was statistically more in the Janus tube, which may be due to the oriented fibers inside the Janus tube promoting the local cell dispersal and migration. In contrast, the control and net patch groups had lower scores and less collagen I deposition on the fibers. Moreover, the expressions of collagen type I and type III in different groups were analyzed by immunofluorescence staining, in which the percentage of collagen I expression was significantly higher in the tube group, compared with the other two groups (Figure S4).

The rat gait recovery is a key postoperative functional analysis item for tendon repair.[28] As shown in Figure 5A−C, the Janus tube group had a larger attaching area and showed a better display of foot shape. The related print area counting showed that the Janus tube group had a significantly larger

https://doi.org/10.1021/acs.nanolett.4c01540
Nano Lett. 2024, 24, 7381−7388

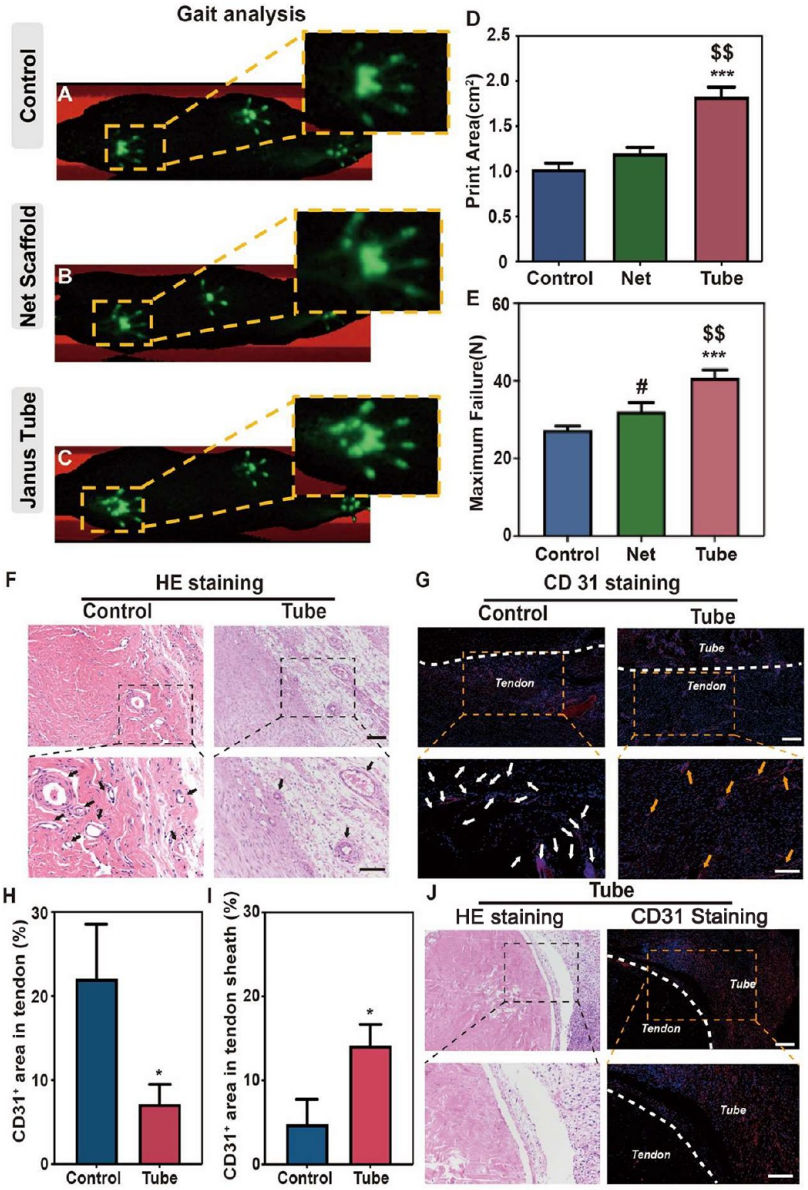

Figure 5. Assessment of Achilles tendon motor function and the histologic characteristics in the early phase of tendon healing. (A−C) Gait analysis of the repaired tendon at 4 weeks. (D) The printing area of the gait analysis (mean ± SD; Janus tube vs control, *** $P < 0.001$; Janus tube vs net scaffold, $$ $P < 0.01$; $n = 3$). (E) Comparison of maximum failure force between experimental groups. (F) H&E staining images of different scaffolds after 7 days. (bar = 100 μm) (mean ± SD; Janus tube vs control, *** $P < 0.001$; Janus tube vs net scaffold, $$ $P < 0.01$; net scaffold vs control, # $P < 0.05$; $n = 3$). (G) CD31 immunofluorescence staining for observing distribution of blood vessels in the tendon (bar = 100 μm). (H,I) Analysis of CD31 marked neovascularization patterns within and adjacent to the tendon sheath in different groups (Janus tube vs control, *$P <$ 0.05; $n = 3$). (J) H&E staining and CD31 immunofluorescence staining of tendon cross-section in different groups (bar = 100 μm).

attaching area than the net scaffold and control groups (Figure 5D). These demonstrated that the Janus tube could promote rat lower limb recovery after tendon repair. Picrosirius red staining was performed to observe the tendon fiber alignment and collagen distribution after repair (Figure S5). In the control group, collagen types I and III were mixed, the tendon fiber orientation was disorganized, and the content and fiber orientation net patch groups would improve more. Furthermore, type I collagen fibers in the Janus group were arranged in dense, parallel arrays, and almost no type III collagen was contained. A biomechanical test further proved the Picrosirius red staining results, in which the Janus tube group had a greater failure force compared with the other two groups (Figure 5E). Therefore, this Janus scaffold was able to promote tendon tissue repair and could inhibit overcellular and scar fiber ingrowth based on the previous experiments, suggesting that this Janus scaffold could balance endogenous and exogenous tendon repair.

To further determine the effect of different types of patches on collagen production at the tendon healing site, immunofluorescence staining was performed on the tendon injury site section at 7 days postoperation. As shown in Figure 5F, the longitudinal section of the Janus tube group, compared to the control group, were less adhered between the tendon and scaffold. Besides that, there was more neovascularity in the tendon tissue of the control group, as marked by the black arrow, and neovascularity in the peritendinous tissue of the Janus tube group, as marked by the white arrow. This result is

https://doi.org/10.1021/acs.nanolett.4c01540
Nano Lett. 2024, 24, 7381−7388

consistent with the electron microscopy finding obtained from an isolated cell culture, demonstrating that the interlaced fiber structure in the outer layer can prevent excessive cell infiltration. There were more angiogenesis processes in the Janus tube group, which were observed and analyzed by angiogenesis marker CD31 immunofluorescence staining, as shown in Figure 5G. Finally, a quantitative analysis of the angiogenesis also demonstrated that the Janus tube could induce early angiogenesis and was nearly present in the inner scaffold and did not grow excessively into the interior of the tendon tissue, as shown in Figure 5H,I. Moreover, some vascular tissue infiltrated the inside of the scaffold to form a vascularized area. Combined with the results of tissue regeneration, it was proved that the tube structure could not only avoid the ingrowth of excessive vascular and scar tissue but also enrich vascular tissue in scaffold structures, which would secrete the corresponding substances required for growth to promote regeneration. The results suggested that the Janus tube could support the tissue space for neovascularization and avoid the direct growth of blood vessels into the tendon. Comparable to the fabrication of prevascularized scaffolds, this technique involves scaffold implantation into the tissue to enrich the vascular tissue prior to reimplantation into the target repair area.[29] Furthermore, the cross section of the Janus group showed a small gap around the tendon and scaffold in the early repair process, as shown in Figure 5 J. As a result, the biofilter tube could enhance tendon tissue regeneration and prevent the ingrowth of scar tissue to promote scarless tendon regeneration.

In the present study, biofilter tube scaffolds with anisotropic structure were successfully fabricated for the first time to induce tendon repair and prevent scar tissue penetration during the repair process. We demonstrated that the inner oriented topographical structures could enhance tenocyte biological behaviors including adhesion, migration, and orientation under a shear force simulation. The outer interlocking fiber could prevent scars and allow vascular tissue penetration to provide a local neovascularization environment. Hence, our study strongly supported the notion that the Janus tube scaffold system employed in this investigation constitutes an innovative topographical approach for tendon repair. This approach focused on regenerating structural anisotropy between the inner and outer bilayers, indicating a novel strategy in the field.

■ ASSOCIATED CONTENT

Supporting Information

The Supporting Information is available free of charge at https://pubs.acs.org/doi/10.1021/acs.nanolett.4c01540.

Materials and methods containing an extended explanation of the fabrication procedure, characterization of material, and the in vitro and in vivo experimental procedure, maximum failure of net and Janus tube groups, SEM micrographs of the net patch scaffold, the live/dead staining results of different groups, immunofluorescence staining of ColI and ColIII, Picrosirius red staining of the different groups, tendon repair assessment scores, and the adhesion histological scoring system (PDF)

■ AUTHOR INFORMATION

Corresponding Authors

Liuquan Yang − *School of Mechanical Engineering, University of Leeds, Leeds LS2 9JT, U.K.*; Email: l.q.yang@leeds.ac.uk

Wenguo Cui − *Shanghai Key Laboratory for Prevention and Treatment of Bone and Joint Diseases, Department of Orthopedics, Sports Medicine Center, Shanghai Institute of Traumatology and Orthopaedics, Ruijin Hospital, Shanghai Jiao Tong University School of Medicine, Shanghai 200025, People's Republic of China*; orcid.org/0000-0002-6938-9582; Email: wgcui80@hotmail.com

Lei Wang − *Shanghai Key Laboratory for Prevention and Treatment of Bone and Joint Diseases, Department of Orthopedics, Sports Medicine Center, Shanghai Institute of Traumatology and Orthopaedics, Ruijin Hospital, Shanghai Jiao Tong University School of Medicine, Shanghai 200025, People's Republic of China*; Email: ray_wangs@hotmail.com

Authors

Renhao Yang − *Shanghai Key Laboratory for Prevention and Treatment of Bone and Joint Diseases, Department of Orthopedics, Sports Medicine Center, Shanghai Institute of Traumatology and Orthopaedics, Ruijin Hospital, Shanghai Jiao Tong University School of Medicine, Shanghai 200025, People's Republic of China*

Yidong Xu − *Shanghai Key Laboratory for Prevention and Treatment of Bone and Joint Diseases, Department of Orthopedics, Sports Medicine Center, Shanghai Institute of Traumatology and Orthopaedics, Ruijin Hospital, Shanghai Jiao Tong University School of Medicine, Shanghai 200025, People's Republic of China*

Renxuan Li − *Shanghai Key Laboratory for Prevention and Treatment of Bone and Joint Diseases, Department of Orthopedics, Sports Medicine Center, Shanghai Institute of Traumatology and Orthopaedics, Ruijin Hospital, Shanghai Jiao Tong University School of Medicine, Shanghai 200025, People's Republic of China*

Yin Zhang − *Shanghai Key Laboratory for Prevention and Treatment of Bone and Joint Diseases, Department of Orthopedics, Sports Medicine Center, Shanghai Institute of Traumatology and Orthopaedics, Ruijin Hospital, Shanghai Jiao Tong University School of Medicine, Shanghai 200025, People's Republic of China*; orcid.org/0000-0001-6810-6280

Yang Xu − *Shanghai Key Laboratory for Prevention and Treatment of Bone and Joint Diseases, Department of Orthopedics, Sports Medicine Center, Shanghai Institute of Traumatology and Orthopaedics, Ruijin Hospital, Shanghai Jiao Tong University School of Medicine, Shanghai 200025, People's Republic of China*

Complete contact information is available at: https://pubs.acs.org/10.1021/acs.nanolett.4c01540

Author Contributions

The manuscript was written through contributions of all authors.All authors have given approval to the final version of the manuscript.

Author Contributions

[§]Renhao Yang, Yidong Xu, and Renxuan Li contributed equally to this work.

https://doi.org/10.1021/acs.nanolett.4c01540
Nano Lett. 2024, 24, 7381−7388

Notes

The authors declare no competing financial interest.

■ ACKNOWLEDGMENTS

This work was supported by the National Natural Science Foundation of China (32171317) and Key project of "Star of Jiaotong University" Biomedical Engineering Foundation (YG2021ZD06).

■ REFERENCES

(1) Nourissat, G.; Berenbaum, F.; Duprez, D. Tendon injury: from biology to tendon repair. *Nat. Rev. Rheumatol* **2015**, *11* (4), 223−233.
(2) Titan, A. L.; Longaker, M. T. A fine balance in tendon healing. *Nat. Cell Biol.* **2019**, *21* (12), 1466−1467.
(3) Maffulli, N.; Moller, H. D.; Evans, C. H. Tendon healing: can it be optimized? *Br J. Sports Med.* **2002**, *36* (5), 315−316.
(4) Deng, B.; Xu, P.; Zhang, B.; Luo, Q.; Song, G. COX2 Enhances Neovascularization of Inflammatory Tenocytes Through the HIF-1alpha/VEGFA/PDGFB Pathway. *Front Cell Dev Biol.* **2021**, *9*, 670406.
(5) Li, Y. W.; Ma, C. H.; Huang, H. K.; Lin, K. J.; Wu, C. H.; Tu, Y. K. Use of Silicone Tubes as Antiadhesion Devices in a Modified Two-Stage Flexor Tendon Reconstruction in Zone II: A Retrospective Study. *J. Hand Surg Am.* **2023**, *48* (5), 444−451.
(6) Karthik, K. K.; Cheriyan, B. V.; Rajeshkumar, S.; Gopalakrishnan, M. A review on selenium nanoparticles and their biomedical applications. *Biomedical Technology* **2024**, *6*, 61−74.
(7) Wang, W.; Hu, Z.; Mo, W.; Ouyang, M.; Lin, S.; Li, X.; Wang, C.; Yu, F.; Wang, Y.; Zhou, D. Ultrastable in-situ silver nanoparticle dressing for effective prevention and treatment of wound infection in emergency. *Engineered Regeneration* **2024**, *5* (1), 111−123.
(8) Zhang, Z.; Zhou, J.; Liu, C.; Zhang, J.; Shibata, Y.; Kong, N.; Corbo, C.; Harris, M. B.; Tao, W. Emerging biomimetic nanotechnology in orthopedic diseases: progress, challenges, and opportunities. *Trends Chem.* **2022**, *4* (5), 420−436.
(9) Xu, Y.; Saiding, Q.; Zhou, X.; Wang, J.; Cui, W.; Chen, X. Electrospun fiber-based immune engineering in regenerative medicine. *Smart Medicine* **2024**, *3* (1), No. e20230034.
(10) Liu, X.; Zhu, B.; Li, Y.; Liu, X.; Guo, S.; Wang, C.; Li, S.; Wang, D. The Role of Vascular Endothelial Growth Factor in Tendon Healing. *Front Physiol* **2021**, *12*, 766080.
(11) Vermeulen, S.; Vasilevich, A.; Tsiapalis, D.; Roumans, N.; Vroemen, P.; Beijer, N. R. M.; Dede Eren, A.; Zeugolis, D.; de Boer, J. Identification of topographical architectures supporting the phenotype of rat tenocytes. *Acta Biomater* **2019**, *83*, 277−290.
(12) Szczesny, S. E.; Elliott, D. M. Interfibrillar shear stress is the loading mechanism of collagen fibrils in tendon. *Acta Biomater* **2014**, *10* (6), 2582−2590.
(13) Loewner, S.; Heene, S.; Baroth, T.; Heymann, H.; Cholewa, F.; Blume, H.; Blume, C. Recent advances in melt electro writing for tissue engineering for 3D printing of microporous scaffolds for tissue engineering. *Front Bioeng Biotechnol* **2022**, *10*, 896719.
(14) Mu, J.; Luo, D.; Li, W.; Ding, Y. Multiscale polymeric fibers for drug delivery and tissue engineering. *Biomedical Technology* **2024**, *5*, 60−72.
(15) Qian, S.; Wang, J.; Liu, Z.; Mao, J.; Zhao, B.; Mao, X.; Zhang, L.; Cheng, L.; Zhang, Y.; Sun, X.; Cui, W. Secretory Fluid-Aggregated Janus Electrospun Short Fiber Scaffold for Wound Healing. *Small* **2022**, *18* (36), No. e2200799.
(16) Zhang, X.; Lv, R.; Chen, L.; Sun, R.; Zhang, Y.; Sheng, R.; Du, T.; Li, Y.; Qi, Y. A Multifunctional Janus Electrospun Nanofiber Dressing with Biofluid Draining, Monitoring, and Antibacterial Properties for Wound Healing. *ACS Appl. Mater. Interfaces* **2022**, *14* (11), 12984−13000.
(17) Zhang, Q.; Yang, Y.; Suo, D.; Zhao, S.; Cheung, J. C.; Leung, P. H.; Zhao, X. A Biomimetic Adhesive and Robust Janus Patch with Anti-Oxidative, Anti-Inflammatory, and Anti-Bacterial Activities for Tendon Repair. *ACS Nano* **2023**, *17* (17), 16798−16816.
(18) Zhang, X.; Li, Q.; Li, L.; Ouyang, J.; Wang, T.; Chen, J.; Hu, X.; Ao, Y.; Qin, D.; Zhang, L.; Xue, J.; Cheng, J.; Tao, W. Bioinspired Mild Photothermal Effect-Reinforced Multifunctional Fiber Scaffolds Promote Bone Regeneration. *ACS Nano* **2023**, *17* (7), 6466−6479.
(19) Zhang, Q.; Zhu, J.; Fei, X.; Zhu, M. A Janus nanofibrous scaffold integrated with exercise-driven electrical stimulation and nanotopological effect enabling the promotion of tendon-to-bone healing. *Nano Today* **2024**, *55*, 102208.
(20) Zhang, X.; Wang, T.; Zhang, Z.; Liu, H.; Li, L.; Wang, A.; Ouyang, J.; Xie, T.; Zhang, L.; Xue, J.; Tao, W. Electrical stimulation system based on electroactive biomaterials for bone tissue engineering. *Mater. Today* **2023**, *68*, 177−203.
(21) Fu, X.; Wang, J.; Qian, D.; Xi, L.; Chen, L.; Du, Y.; Cui, W.; Wang, Y. Oxygen Atom-Concentrating Short Fibrous Sponge Regulates Cellular Respiration for Wound Healing. *Adv. Fiber Mater.* **2023**, *5* (5), 1773−1787.
(22) Passini, F. S.; Jaeger, P. K.; Saab, A. S.; Hanlon, S.; Chittim, N. A.; Arlt, M. J.; Ferrari, K. D.; Haenni, D.; Caprara, S.; Bollhalder, M.; Niederost, B.; Horvath, A. N.; Gotschi, T.; Ma, S.; Passini-Tall, B.; Fucentese, S. F.; Blache, U.; Silvan, U.; Weber, B.; Silbernagel, K. G.; Snedeker, J. G. Shear-stress sensing by PIEZO1 regulates tendon stiffness in rodents and influences jumping performance in humans. *Nat. Biomed Eng.* **2021**, *5* (12), 1457−1471.
(23) Kondratko-Mittnacht, J.; Lakes, R.; Vanderby, R., Jr Shear loads induce cellular damage in tendon fascicles. *J. Biomech* **2015**, *48* (12), 3299−3305.
(24) Vazquez, K.; Saraswathibhatla, A.; Notbohm, J. Effect of substrate stiffness on friction in collective cell migration. *Sci. Rep* **2022**, *12* (1), 2474.
(25) Schulz, C.; Vukicevic, R.; Kruger-Genge, A.; Neffe, A. T.; Lendlein, A.; Jung, F. Monolayer formation and shear- resistance of human vein endothelial cells on gelatin-based hydrogels with tailorable elasticity and degradability. *Clin Hemorheol Microcirc* **2017**, *64* (4), 699−710.
(26) Atcha, H.; Jairaman, A.; Holt, J. R.; Meli, V. S.; Nagalla, R. R.; Veerasubramanian, P. K.; Brumm, K. T.; Lim, H. E.; Othy, S.; Cahalan, M. D.; Pathak, M. M.; Liu, W. F. Mechanically activated ion channel Piezo1 modulates macrophage polarization and stiffness sensing. *Nat. Commun.* **2021**, *12* (1), 3256.
(27) Ito, Y.; Toriuchi, N.; Yoshitaka, T.; Ueno-Kudoh, H.; Sato, T.; Yokoyama, S.; Nishida, K.; Akimoto, T.; Takahashi, M.; Miyaki, S.; Asahara, H. The Mohawk homeobox gene is a critical regulator of tendon differentiation. *Proc. Natl. Acad. Sci. U. S. A.* **2010**, *107* (23), 10538−10542.
(28) Wang, J.; Wang, L.; Gao, Y.; Zhang, Z.; Huang, X.; Han, T.; Liu, B.; Zhang, Y.; Li, Y.; Zhang, L. Synergistic Therapy of Celecoxib-Loaded Magnetism-Responsive Hydrogel for Tendon Tissue Injuries. *Front Bioeng Biotechnol* **2020**, *8*, 592068.
(29) Zhu, W.; Qu, X.; Zhu, J.; Ma, X.; Patel, S.; Liu, J.; Wang, P.; Lai, C. S.; Gou, M.; Xu, Y.; Zhang, K.; Chen, S. Direct 3D bioprinting of prevascularized tissue constructs with complex microarchitecture. *Biomaterials* **2017**, *124*, 106−115.

https://doi.org/10.1021/acs.nanolett.4c01540
Nano Lett. 2024, 24, 7381−7388